Structure and Dimensions of PAMAM/PEG Dendrimer−Star Polymers

Ronald C. Hedden* and Barry J. Bauer

Polymers Division, National Institute of Standards and Technology, Gaithersburg, Maryland 20899

Received October 18, 2002; Revised Manuscript Received December 20, 2002

ABSTRACT: Dendrimer−star polymers are prepared by grafting monofunctional poly(ethylene glycol) (PEG) chains of low polydispersity onto the terminal groups of poly(amidoamine) (PAMAM) dendrimers. A novel gel permeation chromatography technique is used to calculate the average number of PEG branches ("arms") per star. The maximum number of PEG arms (of M_n = 5000 g mol^{-1}) ranges from about 30 arms for a generation 3 dendrimer−star to about 750 arms for a generation 10 dendrimer−star. Radii of gyration of the stars are measured in dilute solution in a good solvent (methanol-d_4) by small-angle neutron scattering (SANS). The stars have measured radii of gyration of about 6−14 nm. Theoretical dimensions of the stars in dilute solution in a good solvent are calculated by treating the stars as a shell of linear chains tethered to a spherical core. The radii of gyration computed from the core−shell model are consistent with the dilute solution values from SANS.

Introduction

Starlike macromolecules (stars, or star-branched polymers) are branched polymers consisting of multiple linear polymer "arms" attached to a core. Recently, stars with increasingly high functionality (number of arms) have been prepared using dendrimers as cross-link junctions.[1−6] Dendrimers are highly branched polymers with a layered, treelike structure that can have reactive end groups. Attachment of monofunctional telechelic polymers to the end groups results in a starlike copolymer that can theoretically have a number of arms f equal to the number of end groups. Because dendrimers may have hundreds or thousands of end groups, it is possible to prepare dendrimer−stars with $f \gg 100$.

Stars of high f can be visualized as "soft" colloids[7] or as spherical polymer brushes.[8] The physical properties of multifunctional stars have been the subject of extensive experimental and theoretical work[9] due to a desire to further understand the physics of soft colloids and polymer brushes. Dendrimer−stars are also of practical interest because they combine the structural properties of a multifunctional star with the chemical properties of the dendrimer. Dendrimer−stars are studied as probe molecules,[10] as stabilizers for colloids,[11] and for DNA delivery.[12]

This report describes the preparation and structural characterization of many-arm poly(ethylene glycol) (PEG) stars with poly(amidoamine) (PAMAM) dendrimers as cores. PAMAM/PEG stars are prepared by grafting monofunctional linear PEG of low polydispersity onto the end groups of PAMAM dendrimers of varying generation, G ($3 < G < 10$). PAMAM/PEG stars have been synthesized previously,[4,5] but this report is the first systematic documentation of their structure and dimensions.

Experimental Section[25]

PAMAM/PEG Star Synthesis. PAMAM/PEG stars were prepared by reaction of *O*-[2-(vinylsulfonyl)ethyl]-*O*′-methylpoly(ethylene glycol) 5000 (Fluka), hereafter called "PEG-VS," with amine-functionalized poly(amidoamine) (PAMAM) dendrimers.[4] The monofunctional PEG-VS arms had reported molecular mass of M_n = 5000 g mol^{-1} and M_w/M_n = 1.01. The sample contained a small percentage of an inert linear PEG dimer. PAMAM generations 3 and 4 Starburst dendrimers with amine end groups were obtained from Aldrich, Inc. (10%/mass in methanol). PAMAM generation 5−10 dendrimers (approximately 25%/mass in methanol) were donated by Dendritech, Inc. PEG-VS arms were attached to the dendrimer terminal $-NH_2$ groups via Michael addition in methanol (J.T. Baker). The mass fraction of combined polymers in the methanol was fixed to 20 ± 2% during the reaction. The Michael reaction proceeded at 22 ± 2 °C for 30 days or more before further use of the stars.

Star Characterization by Gel Permeation Chromatography (GPC). Stars were characterized by gel permeation chromatography using Phenomenex GFC-P-4000 and GFC-P-3000 columns in series with 99.9% water/0.1% triethylamine (by volume) as the mobile phase. An Alltech ELSD 500 evaporative light scattering detector (hereafter called "mass evaporative detector") was used to monitor the column effluent.

Small-Angle Neutron Scattering (SANS). SANS experiments were conducted on dilute solutions of 0.01 ± 0.0001 mass fraction of combined polymers in methanol-d_4 (99.8+ atom % d, Cambridge Isotope Laboratories). Most samples contained some excess linear PEG-VS in addition to the stars. Therefore, the total mass fraction of polymers (stars + excess PEG) was the same for each sample, whereas the mass fraction of stars varied depending on the fractional conversion of PEG to stars. For the G10 star sample, samples of three additional lower concentrations were studied to check for concentration dependence in the scattering.

SANS measurements were conducted at the National Institute of Standards and Technology Center for Cold Neutron Research 8m facility.[13,14] A sample-to-detector distance of 384 cm was employed. The neutron wavelength was λ = 10 Å with a spread of $\Delta\lambda/\lambda$ = 0.12. Data processing was conducted on a μVAX 4000 computer with the software provided by the Center for Neutron Research at NIST.[15] The number of counts was corrected for detector sensitivity, background scattering, and empty cell effects. Absolute scattering intensities were calculated by use of a silica standard and the experimental values for sample transmissions. The resulting data sets were circularly averaged to yield absolute scattering intensity I as a function of scattering vector, q. The incoherent scattering from a cell loaded with methanol-d_4 was measured to estimate the incoherent scattering due to the solvent. The incoherent scattering from the stars was estimated from their hydrogen content and subtracted from the data.

The uncertainties in the scattering data are calculated as the estimated standard deviation of the mean. The total combined uncertainty is not given, as comparisons are made

* Corresponding author: tel 301-975-4356; fax 301-975-3928; e-mail ronald.hedden@nist.gov.

10.1021/ma025752n
Published on Web 02/22/2003

Table 1. GPC Characterization of Dendrimer−Stars

sample	dendrimer generation G	fractional PEG conversion to arms, x	no. of PEG arms f	no. of dendrimer end groups,[a] Z	core mass M_c (g mol^{-1})	star M_n (g mol^{-1})
G3-30	3	0.87 ± 0.05	30 ± 1	32	6.91×10^3	$(1.6 \pm 0.1) \times 10^5$
G4-60	4	0.86 ± 0.05	60 ± 3	64	1.42×10^4	$(3.1 \pm 0.2) \times 10^5$
G5-88	5	0.68 ± 0.05	88 ± 4	128	2.88×10^4	$(4.7 \pm 0.2) \times 10^5$
G6-160	6	0.64 ± 0.05	163 ± 8	256	5.80×10^4	$(8.7 \pm 0.4) \times 10^5$
G7-235	7	0.46 ± 0.05	235 ± 13	512	1.16×10^5	$(1.3 \pm 0.1) \times 10^6$
G8-284	8	0.28 ± 0.05	284 ± 14	1024	2.33×10^5	$(1.7 \pm 0.1) \times 10^6$
G9-460	9	0.22 ± 0.05	460 ± 20	2048	4.67×10^5	$(2.8 \pm 0.1) \times 10^6$
G10-750	10	0.18 ± 0.05	750 ± 40	4096	9.35×10^5	$(4.7 \pm 0.2) \times 10^6$

[a] Theoretical.

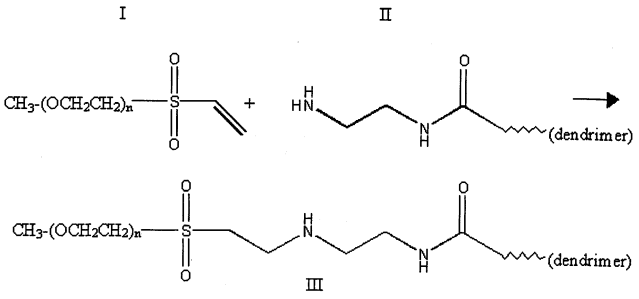

Figure 1. Grafting of PEG-VS onto PAMAM dendrimer end groups by Michael addition.

with data obtained under the same conditions. In cases where the limits are smaller than the plotted symbols, the limits are left out for clarity. Fits of the scattering data were made by a least-squares fit, giving an average and a standard deviation to the fit. The relative uncertainties reported are one standard deviation, based on the goodness of the fit.

Results and Discussion

Dendrimer Generation and Maximum Star Functionality. PAMAM/PEG dendrimer−star polymers were prepared by grafting of monofunctional PEG-VS onto the primary amine end groups of PAMAM dendrimers (Figure 1). The Michael addition reaction of the vinyl sulfone group (I) with the primary amine end groups (II) forms stable secondary amine linkages (III). This preparation of multiarm stars is simpler and more readily accessible than traditional syntheses involving anionic polymerizations.[9] The maximum number of PEG-VS arms that can be attached to a PAMAM-NH_2 dendrimer effectively equals the number of surface primary amines. Reaction of the PEG-VS with a less nucleophilic internal PAMAM amide or a second reaction with an amine end group is less likely.

The maximum number of PEG "arms" that can be attached to a given PAMAM dendrimer is limited by the number of dendrimer end groups, Z. The number of end groups increases exponentially with the number of monomer layers in the dendrimer (called "generations," G, abbreviated G1, G2, etc.). The Starburst PAMAM dendrimers in this study have a tetrafunctional ethylenediamine core, and the expected value of Z is given by

$$Z = 2^{(G+2)} \quad (1)$$

The largest PAMAM studied in this report is G10, which has $Z = 4096$. Values of Z for other generations are listed in Table 1.

Determination of Maximum Star Functionality. Synthesis experiments were designed to establish the maximum number of PEG arms that can be attached to a PAMAM dendrimer of given generation. To maximize f, PAMAM dendrimers of G3 through G10 were reacted with PEG-VS for an extended period of time. For the G3 and G4 samples, a 1.1:1.0 mole ratio of (PEG-VS:PAMAM terminal amines groups) was employed on the basis of the expected number of PAMAM end groups and the molecular mass of the PEG-VS quoted by the supplier. For all other samples the mole ratio of (PEG-VS:amines) was fixed to 1:1.

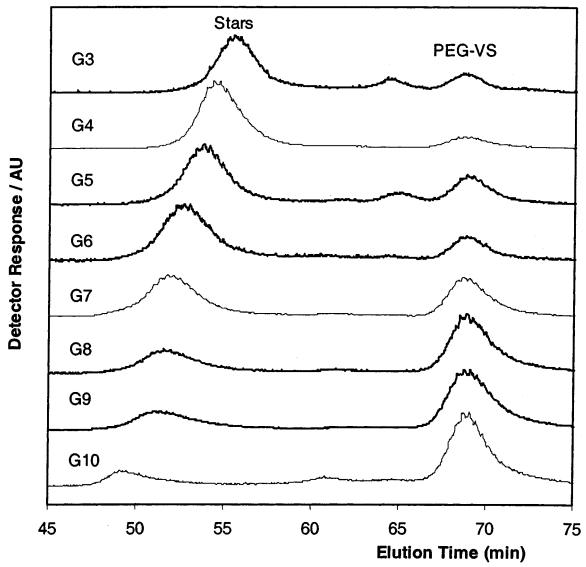

Figure 2. Mass evaporative detector traces from gel permeation chromatography of PAMAM/PEG stars after at least 30 days reaction time.

The conversion of PAMAM dendrimers and PEG-VS to PAMAM/PEG stars was quantified by aqueous GPC. Figure 2 shows GPC mass evaporative detector traces for each of the reaction mixtures after 30 days or more of reaction. At this point, the reaction mixtures had reached a state where further conversion of PEG-VS to star arms was not observed. Repeating the GPC experiments after an additional 30 days produced essentially the same traces. The grafting reaction kinetics can be characterized by recording GPC traces as a function of reaction time.[4] Quantification of the reaction kinetics was not the focus of the present investigation, however, and it was sufficient to note that the reaction reached a practical limit after 30 days.

In Figure 2, the peaks at shorter elution times are due to the star molecules, and the peaks at longer elution time are due to excess PEG-VS. A small amount of an inert PEG "dimer" was sometimes present in the PEG-VS starting material, the amount of which varied slightly between batches. The PEG dimer is visible between the star peak and the PEG-VS peak in the G3 and G5 samples in Figure 2. Because the amount of the dimer was small, its effect was generally negligible in the data analysis.

Complete separation of the star peak from the excess PEG-VS was noted, permitting quantitative determination of the fractional conversion of PEG-VS to stars from the integrated intensities of the mass evaporative detector peaks. Prior to integration, mass evaporative detector response was corrected for its nonlinear dependence on solute concentration. Let w_{PEG} be the mass fraction of PEG in the original reaction mixture, M_c the molar mass of the dendrimer core, M_{PEG} the molar mass of the PEG arms, A_{star} the area of the star elution peak, and A_{PEG} the area of the excess PEG peak. The number of moles of excess PEG arms is given by

$$\text{moles unreacted PEG} = K\frac{A_{PEG}}{M_{PEG}} \tag{2}$$

where K is a proportionality constant relating peak area to mass. The number of moles of reacted PEG (arms) is given by the total moles of PEG minus the moles excess PEG,

$$\text{moles PEG arms} = K(A_{star} + A_{PEG})\left(\frac{w_{PEG}}{M_{PEG}}\right) - K\frac{A_{PEG}}{M_{PEG}} \tag{3}$$

The moles of dendrimers is given by the total mass of dendrimers in the reaction mixture divided by the dendrimer molar mass

$$\text{moles dendrimers} = K(A_{star} + A_{PEG})\frac{1 - w_{PEG}}{M_c} \tag{4}$$

The fractional conversion of PEG-VS to star arms x is given by

$$x = 1 - \frac{A_{PEG}}{(A_{star} + A_{PEG})w_{PEG}} \tag{5}$$

The average number of arms per star f is equal to the moles PEG arms divided by the moles dendrimers. Dividing eq 3 by eq 4 gives

$$f = \left(\frac{(A_{PEG} + A_{star})w_{PEG} - A_{PEG}}{(A_{star} + A_{PEG})(1 - w_{PEG})}\right)\left(\frac{M_c}{M_{PEG}}\right) = \left(\frac{xw_{PEG}}{1 - w_{PEG}}\right)\left(\frac{M_c}{M_{PEG}}\right) \tag{6}$$

Equation 6 accounts for the fact that part of the star peak area A_{star} is due to the mass of the dendrimer. The apparent fractional conversion of PAMAM end groups to star arms is given by the quantity f/Z, where Z is the number of dendrimer end groups. If the total number of PEG-VS chains in the reaction mixture equals the number of dendrimer end groups ("1:1 stoichiometry"), then $x = f/Z$.

Knowing the number of arms allows computation of the number-average molecular mass. Star molecular mass is calculated as

$$M_n = M_c + f\,M_{PEG} \tag{7}$$

The molecular mass is therefore determined without the use of calibration standards. The molecular masses computed by eq 7 are "number averages", as they reflect the total mass of stars formed divided by the number of dendrimers. Similarly, the number of arms f is also a "number-average" quantity. Determination of a weight-average molecular mass M_w or polydispersity index M_w/M_n could be accomplished by addition of a light scattering detector, but none was available at the time of this study.

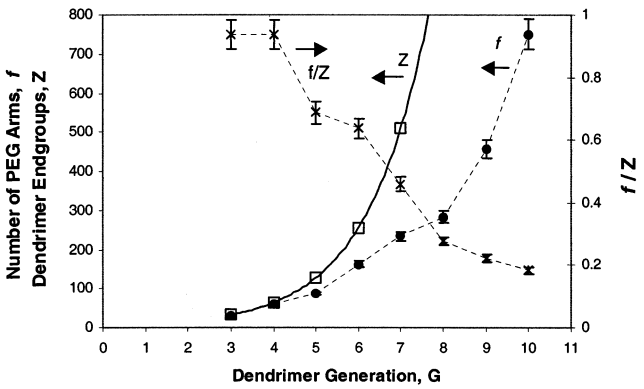

Figure 3. Calculated number of dendrimer end groups Z by eq 1, number of star arms f, and apparent conversion of PAMAM end groups to star arms (f/Z). Lines are guides to the reader's eyes.

The molecular mass distribution of the stars is expected to be relatively narrow. As the grafting reaction proceeds, stars with a deficiency of arms have more reactive sites (free dendrimer end groups) available and offer less steric hindrance to reaction compared to stars with a larger number of arms. These factors tend to narrow the molecular mass distribution, as they favor grafting of additional PEG-VS onto the growing stars with the smallest number of arms. In addition, the maximum molecular mass is constrained by the finite number of dendrimer end groups.

Measured values of x and f are listed in Table 1. The estimated uncertainty in the fractional conversion of arms to stars, x, was estimated as ±5%. Uncertainties in f and M_n are limited by the uncertainty in x and by the values of dendrimer formula weight (M_c) and PEG molar mass (M_{PEG}) quoted by the suppliers. Estimated uncertainties in f are the uncertainty in the measured *average* number of arms but do not describe the width of the molecular mass distribution. Uncertainties quoted are an estimate of one standard deviation of the measurement. Similar uncertainties exist in M_n, which is calculated from f.

The measured values of f range from 30 ± 1 arms for G3 dendrimers to 750 ± 40 arms for G10 dendrimers. The measured value of f approaches the theoretical number of dendrimer end groups Z by eq 1 for the G3 and G4 stars. As generation increases from G5 to G10, the value of f progressively decreases with respect to the calculated value of Z (Figure 3). The quantity f/Z is the apparent conversion of dendrimer end groups to star arms.

All samples contained some excess PEG-VS. The mass fraction of excess PEG-VS and PEG dimer combined varies from about 0.13 for the G3 stars up to 0.82 for the G10 stars. The incomplete reaction of the PAMAM dendrimers with the PEG-VS may be due to steric crowding at the dendrimer surface. As the number density of grafted chains at the dendrimer surface increases, the kinetics of grafting are expected to slow drastically.[4] It is therefore possible that the "equilibrium" number of PEG arms is only an apparent value limited by kinetics. Another possibility is that the dendrimers have fewer amine end groups than the value

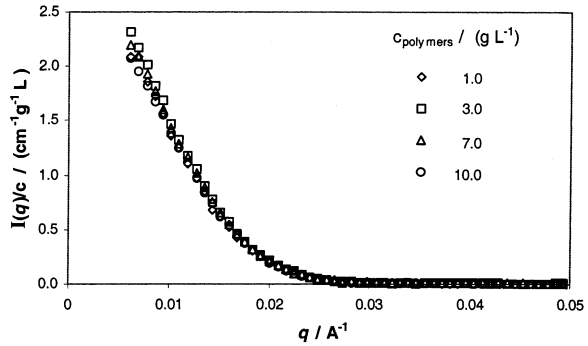

Figure 4. Neutron scattering data for G10-750 stars at four different concentrations.

of Z calculated by eq 1. The PAMAM dendrimers are prepared by repeated sequential addition of ethylenediamine and methyl acrylate monomers to a core. As each generation of monomers is added, a certain amount of defects are introduced due to incomplete reaction or side reactions,[16] causing deviations from the ideal dendrimer structure. The dendrimers are known to contain defects such as loops and missing branches[16] and may have fewer end groups than eq 1 predicts. For dendrimers with a large number of generations, the cumulative effect of these defects may result in a substantial reduction of the number of amine end groups compared to the expected value of Z.

Small-Angle Neutron Scattering in Methanol-d_4 Solution. The goal of the SANS experiments was to quantify star dimensions (radii of gyration, R_g) in dilute solution in a good solvent. Measurements were conducted on the samples listed in Table 1 in dilute methanol-d_4 solutions. The total polymers concentration was 10 g L^{-1} for all samples, including excess PEG-VS (giving a total polymers volume fraction of about 0.01).

Measurement of accurate R_g values for polymers often requires obtaining $I(q)$ vs q data at several different concentrations and extrapolating to zero concentration. We evaluated the importance of concentration effects in this system by studying the most strongly scattering sample, G10-750, at four concentrations. Figure 4 presents the scattering curves obtained for total polymers concentrations ranging from 1.0 to 10.0 g L^{-1}. There was no trend in scattered intensity with decreasing concentration. When R_g was computed for each data set, the values were identical within the limits of experimental precision. We concluded that concentration had little effect on the measured R_g for these dilute star solutions.

In addition to stars, all of the samples contained some excess linear PEG-VS, which contributes to the scattered intensity. The scattered intensity of linear PEG-VS was measured from a 10 g L^{-1} PEG-VS reference solution in methanol-d_4. For each star/PEG mixture, the contribution of the PEG-VS scattering was estimated by multiplying this reference scattering data by the mass fraction of linear material in the sample (determined from GPC analysis). For all of the (star + linear) mixtures, the scattered intensity is dominated by the much larger stars over the q range used for R_g determination. The excess PEG-VS also introduces uncertainty in the star concentration, which affects calculation of absolute intensity. However, determination of star R_g in sufficiently dilute solution does not require knowledge of concentration or absolute intensity. Because our purpose was only to measure star R_g, the linear PEG-VS has little effect on the present study.

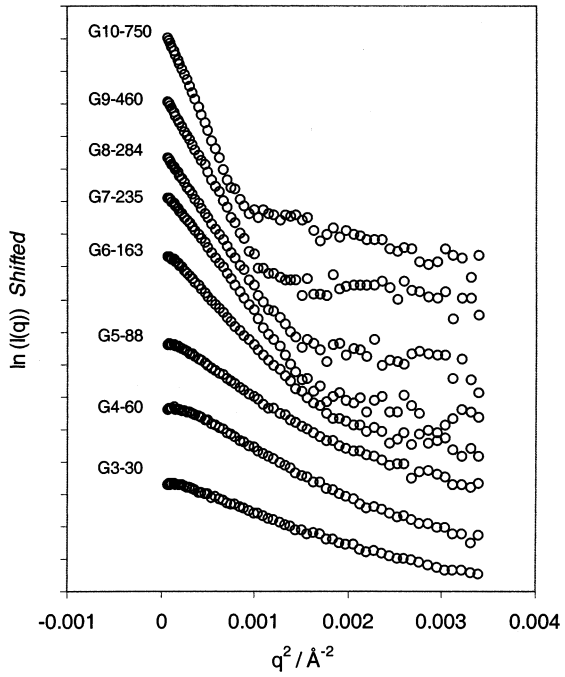

Figure 5. Guinier plots of star SANS data. Data are shifted for clarity.

Table 2. Radii of Gyration Determined by "Guinier" (Eq 8) and "Kratky" (Eq 11) Methods

sample	Guinier R_g (nm)	Kratky R_g (nm)
G3-30	5.67 ± 0.26	6.43 ± 0.32
G4-60	7.06 ± 0.28	7.33 ± 0.37
G5-88	7.67 ± 0.22	8.18 ± 0.41
G6-163	9.73 ± 0.18	10.4 ± 0.5
G7-235	10.6 ± 0.4	11.3 ± 0.6
G8-284	11.4 ± 0.2	12.3 ± 0.6
G9-460	12.5 ± 0.5	13.2 ± 0.7
G10-750	14.3 ± 0.5	14.9 ± 0.7

Analysis of SANS Data by the "Guinier" Approach. R_g may be extracted from $I(q)$ by treating the stars as particles of unspecified size and shape and conducting a Guinier analysis. Stars are assumed to be noninteracting, and the solutions are presumed to be disordered. R_g is extracted from the data using the Guinier approximation.[17]

$$\ln(I(q)) \approx \ln(I(q=0)) - q^2 R_g^2/3 \qquad (8)$$

The data are plotted as $\ln(I(q))$ vs q^2, and R_g is determined from a fit to the linear region at low q. Strictly speaking, eq 8 is an approximation valid only where ($q \ll R_g^{-1}$). However, for quasi-spherical particles, the upper limit of the useful q range is extended because the scattering form factor of a sphere is approximated well by eq 8 even for $q \approx R_g$. Guinier plots for the star solutions are shown in Figure 5, and all of the plots have an approximately linear region at low q. Values of R_g calculated by linear least-squares fits to the linear portion of the scattering curve are reported in Table 2. The selection of the upper bound of the q range for the fit is admittedly somewhat arbitrary, but this is an inherent limitation of the Guinier analysis. Values of R_g range from 5.67 ± 0.26 nm for the G3-30 sample to 14.3 ± 0.5 nm for the G10-750 sample. As expected, the radius of gyration increased progressively as the dendrimer generation (and therefore number of arms) increased.

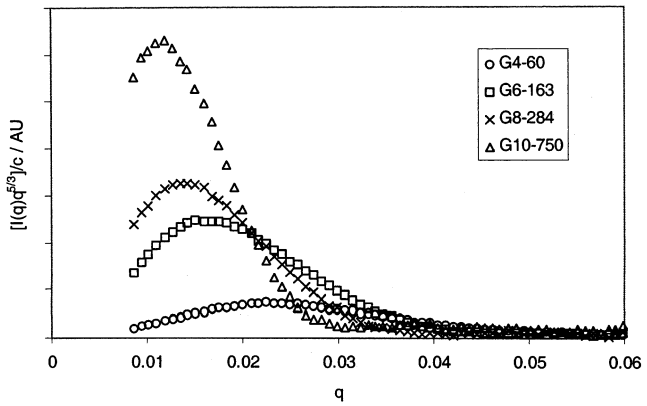

Figure 6. Kratky plots for selected stars.

An improvement to the Guinier expression for star polymers that extends the useful q range was developed by Dozier et al.[18] by addition of a second term describing scattering arising from short-range correlations within a star. However, in the present study, the uncertain effects of the excess linear PEG on the high-q scattering data limited us to use of the simple Guinier approach.

Analysis of SANS Data by the "Kratky" Approach. A second method of determining R_g from a Kratky plot, $I(q)q^{1/\nu}$ vs q, where ν is the excluded-volume parameter. For dilute solutions of stars in a good solvent, $I(q)q^{5/3}$ is plotted vs q, and a peak in the scattered intensity is observed at some scattering vector $q = q_{max}$. The value of q_{max} is determined from experimental data by numerically computing $d[I(q)q^{5/3}]/dq$. The radius of gyration is then calculated by application of the Benoit expression[21] describing the scattering from Gaussian star polymers. The Benoit expression for the single-chain scattering function $P(q)$ is

$$P(q) = \frac{2}{f\upsilon^4}\left(\upsilon^2 - [1 - \exp(-\upsilon^2)] + \frac{f-1}{2}[1 - \exp(-\upsilon^2)]^2\right) \quad (9)$$

where

$$\upsilon = \left(\frac{f}{3f-2}\right)^{1/2} qR_g \quad (10)$$

If the analytical expression eq 9 is plotted as $P(q)\upsilon^{5/3}$ vs υ (for a chosen value of f), a maximum in $P(q)$ occurs at $\upsilon = \upsilon_{max}$. (Alternately, the value of υ_{max} can be determined by setting $d[P(q)\upsilon^{5/3}]/d\upsilon = 0$.) For a large number of branches ($f \gg 1$), $\upsilon_{max} \approx 1$. The value of R_g is then calculated by comparing υ_{max} to the experimentally determined q_{max}. Rearranging eq 10 and evaluating at $q = q_{max}$ yields

$$R_g = \left(\frac{3f-2}{f}\right)^{1/2} \frac{\upsilon_{max}}{q_{max}} \quad (11)$$

or

$$R_g \approx \frac{\sqrt{3}}{q_{max}} \quad (12)$$

when $f \gg 1$. No fit to eq 9 is made; only the measured position of the peak q_{max} is used to estimate R_g.

Kratky plots for the samples G4-60, G6-163, G8-284, and G10-750 are shown in Figure 6. The peaks in the Kratky plots confirm that the scattering arises from starlike structures. The value of the peak position q_{max} decreases as the number of branches and the radius of gyration increase. Radii of gyration calculated by eq 11 are presented in Table 2. Uncertainties in R_g were estimated by assuming an uncertainty of ±5% in q_{max}. The R_g values calculated by the Kratky method are slightly higher than those extracted via the Guinier approach.

The Guinier and Kratky methods differ in the way R_g is extracted from the $I(q)$ vs q data and therefore have different limitations. A primary limitation of the Guinier method is that the selection of the q range for the fit is arbitrary unless data are obtained at very low values of qR_g. The Kratky method assumes that the star arms have Gaussian statistics, ignoring excluded-volume effects that may be present in real stars.

PAMAM-PEG Stars Modeled as Spherical Polymer Brushes. Theoretical dimensions of dendrimer−stars are calculated here on the basis of a polymer brush model. Dendrimer−stars are modeled as a shell of linear chains tethered to a spherical core. The radius of gyration is found by assuming a radial monomer density distribution in the corona. Separate neutron scattering contrast factors are introduced for the core and the shell.

From the definition of the radius of gyration (working in spherical coordinates)

$$R_g^2 = \frac{\int_0^\infty [\rho_n(r)r^2]r^2\,dr}{\int_0^\infty [\rho_n(r)]r^2\,dr} \quad (13)$$

where $\rho_n(r)$ is a radial density distribution function. To estimate R_g for a neutron scattering measurement, $\rho_n(r)$ must be the neutron scattering length density (SLD) distribution. $\rho_n(r)$ is referenced to the background (solvent) because there is no coherent scattering if the polymer SLD matches the solvent SLD. For $\rho_n(r)$, we define three regions: inside the dendrimer, inside the PEG shell, and outside the star, such that

$$\begin{aligned} \rho_n(r) &= \rho_c \qquad r < R_c \\ \rho_n(r) &= k_n r^{(1/\nu)-3} \qquad R_c < r < R \\ \rho_n(r) &= 0 \qquad R < r \end{aligned} \quad (14)$$

R is an effective outer radius of the star, and R_c is the outer radius of the core. For simplicity, the dendrimer core is treated as a solid sphere with a uniform SLD. While the monomer density distribution in a real dendrimer certainly is a function of r, this simplification is reasonable here because the calculated R_g is dominated by the shell of PEG chains. The radial density distribution function in the shell ($R_c < r < R$) is adopted from the scaling analysis (blob model) of Daoud and Cotton.[19] k_n is a scattering contrast constant, and ν is the excluded-volume parameter. $\rho_n(r)$ is assumed to drop sharply to zero at $r = R$ due to the finite extensibility of the tethered chains. In general, $\rho_n(r)$ is also discontinuous at $r = R_c$, as $\rho_n(R_c)$ is not constrained to match ρ_c.

Substituting eq 14 into eq 13

$$R_g^2 = \frac{\int_0^{R_c} \rho_c r^4\,dr + k_n\int_{R_c}^{R} r^{(1/\nu)+3}\,dr}{\int_0^{R_c} \rho_c r^2\,dr + k_n\int_{R_c}^{R} r^{(1/\nu)-1}\,dr} \quad (15)$$

Performing the integrations in eq 15 gives

$$R_g^2 = \frac{\frac{R_c^5 \rho_c}{5} + k_n\left(\frac{\nu}{1+2\nu}\right)(R^{2+(1/\nu)} - R_c^{2+(1/\nu)})}{\frac{R_c^3 \rho_c}{3} + k_n \nu (R^{(1/\nu)} - R_c^{(1/\nu)})} \quad (16)$$

Evaluation of R_g by eq 16 requires expressions for ρ_c, R, and the constant k_n.

The core contrast factor is given by

$$\rho_c = \left(\frac{3}{4\pi R_c^3}\right)\left(\sum_{\text{dendrimer}} b - \left(\frac{\nu_d}{\nu_s}\right)\sum_{\text{solvent}} b\right) \quad (17)$$

where b is the scattering length of a given nucleus, and the sums are taken over an entire dendrimer and a solvent molecule. ν_d and ν_s are the partial molar volumes of a dendrimer and a solvent molecule.

The outer radius of the star R can be computed according to the procedure followed by Vagberg, Cogan, and Gast.[22] The total number of monomers in the outer shell is Nf, where N is the number of statistical monomers per chain,[22] giving

$$4\pi \int_{R_c}^{R} \rho(r) r^2 \, dr = Nf \quad (18)$$

where $\rho(r)$ is the monomer density distribution. The density of monomers in the shell is taken as

$$\rho(r) = k r^{(1/\nu)-3} \quad (19)$$

where k is a normalization constant. k is related to k_n by a factor converting monomer density to scattering length density (referenced to solvent).

$$k_n = k\left(\sum_{\text{monomer}} b - \left(\frac{\nu_p}{\nu_s}\right)\sum_{\text{solvent}} b\right) \quad (20)$$

In eq 20, ν_p is the molar volume of a PEG monomer. Inserting eq 19 into eq 18 and performing the integration gives

$$k\nu(R^{1/\nu} - R_c^{1/\nu}) = \frac{Nf}{4\pi} \quad (21)$$

k can be computed by calculating the monomer density in the outer shell at the surface of the core. According to the analysis presented in ref 22, $\rho(R_c)$ is given by[22]

$$\rho(R_c) = \frac{3}{32\pi}\left(\frac{4}{l}\right)^{1/\nu} R_c^{(1-3\nu)/\nu} f^{(3\nu-1)/2\nu} \quad (22)$$

Here l is the statistical segment length of a monomer. Comparing eq 22 with eq 19 gives

$$k = \left(\frac{3}{32\pi}\right)\left(\frac{4}{l}\right)^{1/\nu} f^{(3\nu-1)/2\nu} \quad (23)$$

and therefore

$$k_n = \left(\sum_{\text{PEG monomer}} b - \left(\frac{\nu_p}{\nu_s}\right)\sum_{\text{solvent}} b\right)\left(\frac{3}{32\pi}\right)\left(\frac{4}{l}\right)^{1/\nu} f^{(3\nu-1)/2\nu} \quad (24)$$

Substituting eq 23 into eq 19, the outer radius of the star R is[22]

$$R = \left(N l^{1/\nu} \frac{8 f^{(1-\nu)/2\nu}}{3\nu 4^{1/\nu}} + R_c^{1/\nu}\right)^{\nu} \quad (25)$$

Theoretical values for R_g can now be computed by eq 16. If the size of the dendrimer is assumed not to change after attachment of the PEG arms, then the core radius R_c is the hydrodynamic radius of the dendrimer in a good solvent. R_c values were taken to be the measured hydrodynamic radii of the dendrimers in methanol.[23] $N = 113$ monomers per arm based on the molar mass of the PEG arms. A monomer statistical length for poly(ethylene glycol) of $l = 0.424$ nm was estimated from published data concerning the dimensions of long poly(ethylene oxide) chains good solvents.[24] A value of 40.2 cm^3 mol^{-1} was taken for ν_p based on the melt density of amorphous poly(ethylene glycol) oligomers at 25 °C.[20] A value of 40.5 cm^3 mol^{-1} was taken for ν_s (methanol-d_4). The molar volume of each dendrimer generation was calculated on the basis of mass density and formula weight quoted by the supplier. Radii of gyration were computed for "good solvent" conditions ($\nu = {}^3/_5$).

Table 3 summarizes the predictions of eq 16. The measured R_g values are in surprisingly good agreement with the calculated values. The measured radii of gyration lie close to the good solvent prediction, suggesting that the 5000 g mol^{-1} PEG chains are sufficiently long to expand due to excluded-volume effects. As the number of PEG arms increases from 30 to 750, the calculated shell thickness ($R - R_c$) increases, indicating an effective stretching of the arms.

Table 3. Calculation of Star Dimensions by the Density Distribution Model

sample	measd R_c (nm)[a]	R_g (nm)	R (nm)	$(R - R_c)$ (nm)
G3-30-5K	1.88 ± 0.01	6.27	9.13	7.25
G4-60-5K	2.30 ± 0.01	7.26	10.5	8.20
G5-88-5K	2.82 ± 0.01	7.94	11.5	8.68
G6-163-5K	3.63 ± 0.01	9.18	13.2	9.57
G7-235-5K	4.19 ± 0.03	9.92	14.3	10.1
G8-284-5K	5.02 ± 0.01	10.5	15.2	10.2
G9-460-5K	5.92 ± 0.01	11.6	16.9	11.0
G10-750-5K	6.99 ± 0.01	12.9	18.9	11.9

[a] Small-angle X-ray scattering data in methanol reproduced from ref 23.

Summary

Starlike polymers with large numbers of arms can be prepared by grafting monofunctional telechelics onto the end groups of dendrimers. This preparation of multiarm stars is straightforward from a synthetic standpoint, but some amount of excess linear material is usually present. The SANS radii of gyration of PAMAM/PEG stars in dilute solution are in reasonable agreement with the predictions of a polymer brush model. The measured star dimensions suggest that the tethered PEG arms of 5000 g mol^{-1} are long enough to expand in a good solvent, even when the number of arms is large.

Acknowledgment. Dr. Hedden acknowledges the support of a National Research Council Research Associateship. We thank Dr. Derek Ho, Dr. John Barker, and Dr. Charles Glinka of the NCNR for assistance with the 8m SANS instrumentation. We acknowledge the support of the National Institute of Standards and Technology, U.S. Department of Commerce, in providing

the neutron research facilities used in this work. We thank Dendritech, Inc., for providing the generation 5−10 PAMAM dendrimers.

References and Notes

(1) Balogh, L.; Leuze-Jallouli, A.; Dvornic, P.; Kunugi, Y. T.; Blumstein, A.; Tomalia, D. A. *Macromolecules* **1999**, *32*, 1036−1042.
(2) Comanita, B.; Noren, B.; Roovers, J. *Macromolecules* **1999**, *32*, 1069−1072.
(3) Roovers, J.; Zhou, L. L.; Toporowski, P. M.; van der Zwan, M.; Iatrou, H.; Hadjichristidis, N. *Macromolecules* **1993**, *26*, 4324−4331.
(4) Viers, B. D.; Bauer, B. J. *Abstr. Pap. Am. Chem. Soc.* **2001**, *221*, 399-PMSE.
(5) Yen, D. R.; Merrill, E. W. *Abstr. Pap. Am. Chem. Soc.* **1997**, *213*, 27-OLY.
(6) Zhou, L. L.; Hadjichristidis, N.; Toporowski, P. M.; Roovers, J. *Rubber Chem. Technol.* **1992**, *65*, 303−314.
(7) Likos, C. N.; Lowen, H.; Watzlawek, M.; Abbas, B.; Jucknischke, O.; Allgaier, J.; Richter, D. *Phys. Rev. Lett.* **1998**, *80*, 4450−4453.
(8) Semenov, A. N.; Vlassopoulos, D.; Fytas, G.; Vlachos, G.; Fleischer, G.; Roovers, J. *Langmuir* **1999**, *15*, 358−368.
(9) Grest, G. S.; Fetters, L. J.; Huang, J. S.; Richter, D. *Adv. Chem. Phys.* **1996**, *94*, 67−163.
(10) Hedden, R. C.; Muzny, C.; Bauer, B. J.; Amis, E. J. Manuscript in preparation.
(11) Hedden, R. C.; Bauer, B. J.; Smith, A. P.; Gröhn, F.; Amis, E. J. *Polymer* **2002**, *43*, 5473−5481.
(12) Luo, D.; Haverstick, K.; Belcheva, N.; Han, E.; Saltzman, W. M. *Macromolecules* **2002**, *35*, 3456−3462.
(13) Hammouda, B.; Krueger, S.; Glinka, C. J. *J. Res. Natl. Inst. Stand. Technol.* **1993**, *98*, 31−46.
(14) Prask, H. J.; Rowe, J. M.; Rush, J. J.; Schroeder, I. G. *J. Res. Natl. Inst. Stand. Technol.* **1993**, *98*, 1−13.
(15) NIST Cold Neutron Research Facility, "SANS Data Reduction and Imaging Software", 1996.
(16) Tomalia, D. A.; Baker, H.; Dewald, J.; Hall, M.; Kallos, G.; Martin, S.; Roeck, J.; Ryder, J.; Smith, P. *Polym. J.* **1985**, *17*, 117−132.
(17) Guinier, A.; Fournet, G. *Small Angle Scattering of X-rays*; Wiley: New York, 1955.
(18) Dozier, W. D.; Huang, J. S.; Fetters, L. J. *Macromolecules* **1991**, *24*, 2810−2814.
(19) Daoud, M.; Cotton, J. P. *J. Phys. (Paris)* **1982**, *43*, 531−538.
(20) *Physical Properties of Polymers Handbook*; American Institute of Physics Press: Woodbury, NY, 1996.
(21) Benoit, H. *J. Polym. Sci.* **1953**, *11*, 507.
(22) Vagberg, L. J. M.; Cogan, K. A.; Gast, A. P. *Macromolecules* **1990**, *24*, 1670−1677.
(23) Prosa, T. J.; Bauer, B. J.; Amis, E. J. *Macromolecules* **2001**, *34*, 4897−4906.
(24) *Polymer Handbook*, 3rd ed.; Wiley: New York, 1989.
(25) Certain commercial materials and equipment are identified in this paper in order to adequately specify the experimental procedure. In no case does such identification imply recommendation by the National Institute of Standards and Technology nor does it imply that the material or equipment is the best available for this purpose.

MA025752N